

Gas-surface scattering with multiple collisions in the physisorption potential well

Guoqing Fan and J. R. Manson

Department of Physics and Astronomy, Clemson University, Clemson, South Carolina 29634, USA

(Received 8 October 2004; revised manuscript received 27 May 2005; published 3 August 2005)

The problem of gas-surface collisions is developed in terms of a theoretical formalism that allows calculations of multiple collisions of particles trapped in the physisorption well. The calculation uses classical dynamics for describing the scattering. Multiple collisions in the well are treated with an iterative process that can be followed to very high order numbers until all trapped particles are desorbed. Example calculations are carried out for scattering in a one-dimensional potential. Two different initial gas distributions are considered, a monoenergetic incident beam and an equilibrium gas appropriate for calculating the energy accommodation coefficient. Each part of the scattered distribution, the directly scattered fraction, the desorbed fraction and the trapped fraction, can be examined separately. The desorbed distribution is often found to deviate significantly from an equilibrium state. This behavior is contrary to long-standing hypotheses in which it is assumed that the trapped-desorbed fraction escapes the surface in an equilibrium distribution at the surface temperature. The energy distribution of the trapped fraction is examined and from it desorption times are calculated. The formalism is used to calculate the equilibrium energy accommodation coefficient, including contributions of desorbing particles. It is found that the effective energy accommodation coefficient of that fraction of the incident beam that is initially trapped and then subsequently desorbed may be less than unity.

DOI: [10.1103/PhysRevB.72.085413](https://doi.org/10.1103/PhysRevB.72.085413)

PACS number(s): 34.50.Dy, 34.50.Pi, 82.20.Rp

I. INTRODUCTION

Maxwell is credited with being the first to introduce the concept of energy accommodation in his work on the scattering of gases from surfaces. He made the simple assumption that a gas impinging on a surface would produce a scattered distribution that could be divided into two fractions, one that exchanges no energy with the surface and the other that equilibrates or accommodates to the temperature of the surface.¹ Early in the twentieth century Knudsen introduced the terminology “coefficient of thermal accommodation” to measure the efficiency of energy exchange at the interface between a gas and a surface and developed firm theoretical foundations for describing it.² Since the work of Knudsen the concept of the accommodation coefficient has become firmly entrenched in the study of gas-surface interactions and finds important applications in areas as diverse as aerodynamics, rocket flight, re-entry of space vehicles into planetary atmospheres, microengines, turbines, and plasma confinement. An extensive literature has been developed on the subject together with several excellent reviews.^{3,4}

The purpose of this paper is to develop a scattering theory for monatomic projectiles colliding with a surface, using classical dynamics, and including trapping-desorption processes in the attractive physisorption well of the interaction potential. Upon initially colliding with the surface a fraction of the gas particles is scattered back into the continuum states, and the remaining fraction is trapped at the surface in the potential well. An iterative method is presented for calculating the subsequent energy exchanges of the initially trapped particles as they continue to move in the well and make multiple collisions with the surface. This iterative process can be followed until essentially all of the initially trapped particles have desorbed.

At the level presented here, the scattering process is treated in one dimension with the attractive interaction con-

sisting of a square well potential. Clearly, a one-dimensional treatment is inadequate for describing a real surface scattering experiment in which a well-defined beam of incident atoms is directed towards a surface. However, there is one type of measurement in which one-dimensional theories have played a role of significance, and this is for calculations of the energy accommodation coefficient. A measurement of the energy accommodation coefficient involves placing a three-dimensional gas in contact with a surface and measuring the total energy exchange. A calculation of such experimental conditions involves, at minimum, three-dimensional integrals over the momenta of the incident as well as the scattered gas. Because such a calculation can be lengthy, there is a long history of using simple one-dimensional models in calculations of the accommodation coefficient.^{3,4} However, even in this case, the use of a one-dimensional model requires some justification because there is ample evidence that scattering in one dimension is not adequate for obtaining quantitative agreement of the energy accommodation coefficient with available experimental data.⁵ However, 1D models often give good qualitative results for predicting the behavior of the energy accommodation coefficient with respect to the available initial parameters such as gas mass m , physisorption potential well depth D , and temperature T . It is for these reasons, and because the calculations require far less computational time for the iteration process developed here, that a 1D model is utilized in these initial theoretical developments. The possibilities for extending these calculations to more realistic fully three-dimensional potentials are briefly discussed below in the conclusions.

The use of classical mechanics to describe the hard-core collision, on the other hand, is justified for many systems of interest in rarefied gas-surface dynamics. A classical treatment means that the results will be valid for heavier mass atoms, high energies, and gases and surfaces at high temperatures where quantum effects are not dominant.

The method for calculating multiple collisions of the initially trapped particles is developed in a manner that is independent of the energy distribution of incident particles colliding with the surface. We carry out numerical calculations for two quite different cases, a monoenergetic incident beam which would correspond to a typical scattering experiment, and an equilibrium incident gas distribution which is the case usually considered in calculations of the energy accommodation coefficient.

Several of the numerical calculations carried out here are for the energy accommodation coefficient. Extensive experimental investigations of the energy accommodation coefficient have been carried out especially in the rarefied gas dynamics regime. Among the most precise and reliable are measurements of the energy accommodation coefficient for the rare gases in contact with a tungsten surface by the groups of Thomas^{6,7} and Menzel.^{8,9} Although these measurements are now rather old, they are still considered reliable and it is this rare gas on tungsten data that is almost always used as a benchmark for comparing the calculated results of theoretical treatments with experiment. Here, we revisit the theory of the energy accommodation coefficient for monatomic gases^{3,4} using classical dynamics for the scattering process and including a full treatment of trapping-desorption processes in the attractive physisorption well of the interaction potential.

In addition to calculations of the accommodation coefficient and energy distributions of scattered particles, this iterative approach allows one to calculate the expected energy distributions of the trapped particles, and to follow the evolution of the trapped energy distribution as the number of repeated collisions with the surface becomes larger. It is found that the trapped energy distribution evolves and then stabilizes after a relatively small number of collisions compared to the time that it takes all particles to be desorbed. After this stabilization, the total fraction of trapped particles decreases but the functional form of their energy distribution remains nearly constant. Knowledge of the energy distribution of the trapped fraction allows calculations of the lifetime of a trapped particle, and values obtained are in reasonable agreement with expectations.

The contents of this paper are organized as follows: in the next section (Sec. II), the iteration model for multiple collisions of the trapped fraction in the potential well is developed, the theory of accommodation coefficient is briefly presented and methods for calculating the time it takes for the trapped particles to desorb are discussed. In Sec. III, the results of the calculations are shown and further discussion and conclusions are given in Sec. IV.

II. THEORY

A. Differential reflection coefficient

The intensity measured in a surface scattering event is the differential reflection coefficient $dR(E_f, E_G)/dE_f$ which gives the probability per unit final energy that a particle of well-defined incident energy E_G will be scattered into the small interval dE_f centered about the final energy E_f . The differential reflection coefficient includes multiple scattering with the

surface. For $E_f > 0$ it gives the intensity scattered into the continuum states while for $E_f < 0$ it gives the intensity scattered into the bound states, i.e., the trapped fraction, which then continues to move in the physisorption well and make further collisions with the surface. In the iteration method developed here, the scattering process starts with an initial collision described by the zeroth order differential reflection coefficient, denoted by $dR^0(E_f, E_G)/dE_f$.

The iteration method developed in Sec. II B below does not, in general, depend on the specific nature of the zeroth order differential reflection coefficient. However, it is useful at this point to specify the scattering model that we will use for all calculations in this paper. A model that has been useful in explaining experimental gas-surface and low-energy ion-surface scattering data is the differential reflection coefficient for an incident particle of mass m in collision with a surface of discrete atomic cores of mass M in the classical limit, which in 1D is given by^{10,11}

$$\frac{dR^0(E_f, E_G)}{dE_f} = \frac{1}{N^0 \sqrt{4\pi k_B T \Delta E_0}} \exp\left(-\frac{(E_f - E_G + \Delta E_0)^2}{4k_B T \Delta E_0}\right), \quad (1)$$

where k_B is the Boltzmann's constant, ΔE_0 is the recoil energy of the collision given by

$$\Delta E_0 = (p_f - p_G)^2 / 2M = \mu(\sqrt{E_f} + \sqrt{E_G})^2, \quad (2)$$

with $\mu = m/M$ the mass ratio and N^0 is a normalization constant chosen such that $\int_0^\infty dE_f dR^0(E_f, E_G)/dE_f = 1$. Equation (1), in its 3D form, has been shown to give good descriptions of surface scattering in systems ranging from rare gases colliding with metals^{12,13} to low energy ion scattering.^{14,15}

B. Iteration method

In order to include a physisorption potential we use a square well of width b and depth D in front of the surface. The leading edge, or attractive part, of the potential is stationary while the repulsive part consists of the 1D mass M , which is vibrating with an equilibrium distribution given by equipartition of energy. The reason for taking the attractive part of the potential to be stationary is based on reasoning for the actual form of the one-dimensional attractive van der Waals potential in front of a real 3D surface which has an asymptotic form at large distances z given by $V(z) \approx -D_3/z^3$, which is static. The reason why the attractive part of the van der Waals potential does not vibrate is because it is the result of a three-dimensional sum over all the atoms in the semi-infinite solid and the summation of the vibrational displacements of this 3D distribution of atoms averages essentially to zero. Thus, since the collision of an incoming gas atom with the repulsive potential occurs inside the well, the differential reflection coefficient of Eq. (1) will be transformed according to $E_{f,G} \rightarrow E'_{f,G} = E_{f,G} + D$. Since this is a classical calculation, there is no quantum mechanical reflection by the attractive step.

After the initial collision with the surface as described by the differential reflection coefficient $dR^0(E'_f, E'_G)/dE'_f$, now written as a function of the energies inside the well, the

energy distribution of the trapped fraction is that for $0 < E'_f < D$ and the distribution of the continuum fraction that escapes the surface is that for $E'_f > D$, which is the same as $E_f > 0$. This becomes the 0th iteration.

The trapped particles continue to bounce back and forth inside the well and each time that a particle collides with the repulsive wall there is a probability that it will gain enough energy to escape into the continuum with $E'_f > D$, otherwise it remains trapped and continues to collide. Eventually all of the particles trapped in the 0th collision will escape. The continued collisions of the particles that remain trapped can be calculated with the following iteration procedure for iteration orders $n \geq 1$:

$$\frac{dR^n(E'_f, E'_G)}{dE'_f} = \begin{cases} \frac{dR^{n-1}(E'_f, E'_G)}{dE'_f} + \frac{dR^n_T(E'_f, E'_G)}{dE'_f}, & E'_f > D, \\ \frac{dR^n_T(E'_f, E'_G)}{dE'_f}, & 0 < E'_f < D, \end{cases} \quad (3)$$

where the n th order differential reflection coefficient is divided into continuum and trapped fractions as before. The n th order differential reflection coefficient for the trapped fraction is given by

$$\frac{dR^n_T(E'_f, E'_G)}{dE'_f} = \int_0^D dE'' \frac{dR^0(E'_f, E'')}{dE'_f} \frac{dR^{n-1}(E'', E'_G)}{dE''}. \quad (4)$$

In Eq. (4), the n th order differential reflection coefficient is obtained as an integral over intermediate energy E'' using the $(n-1)$ th distribution of particles in the well as the source of the incoming distribution. For each intermediate energy, the particles colliding with the surface scatter according to the 0th order differential reflection coefficient. The result is that a fraction is elevated to final energies $E'_f > D$ and escapes, while the remainder stays bound in the well as exhibited in Eq. (3).

After each iteration the differential reflection coefficient of Eq. (3) is renormalized just as in the 0th order case such that

$$\int_0^\infty dE'_f \frac{dR^n(E'_f, E'_G)}{dE'_f} = 1. \quad (5)$$

The fraction of the particles in the continuum state P_C^n and the fraction remaining trapped after the n th iteration P_T^n are

$$P_C^n = \int_0^\infty dE_G \int_D^\infty dE'_f \frac{dR^n(E'_f, E'_G)}{dE'_f} \frac{dP(E_G)}{dE_G}, \quad (6)$$

$$P_T^n = \int_0^\infty dE_G \int_0^D dE'_f \frac{dR^n_T(E'_f, E'_G)}{dE'_f} \frac{dP(E_G)}{dE_G}, \quad (7)$$

where $dP(E_G)/dE_G$ is the energy distribution of particles in the incident beam, also normalized to unity

$$\int_0^\infty dE_G \frac{dP(E_G)}{dE_G} = 1. \quad (8)$$

With the normalization of the differential reflection coefficient of Eq. (5) $P_C^n + P_T^n = 1$, i.e., unitarity is preserved.

The iteration procedure described above is not one that accounts for the fact that the trapped particles with higher energies collide more often than those with lower energies. Instead, this iteration procedure gives an equal number of iterations to particles in each energy interval. Although the higher energy particles are more likely to desorb after a smaller number of iterations, the final continuum distribution will be accurately calculated if the iteration process is carried out to high enough orders that essentially all initially trapped particles are desorbed.

C. Energy accommodation coefficient

The energy accommodation coefficient $\alpha(T_S, T_G)$ as defined by Knudsen is the energy transferred to a surface at temperature T_S in contact with a gas in an equilibrium distribution with temperature T_G , relative to the maximum transfer thermodynamically allowed. It is given by

$$\alpha(T_S, T_G) = \frac{\overline{E_f} - \langle E_G \rangle}{\langle E_S \rangle - \langle E_G \rangle}, \quad (9)$$

where $\langle E_{G,S} \rangle$ is the average energy of the flux of particles crossing a plane in an equilibrium gas of temperature T_G or T_S , respectively, and E_f is the average energy of a particle reflected from the surface.

Since this paper will use a 1D model, the Knudsen flux distribution (Maxwell-Boltzmann distribution with the streaming correction) expressed as the probability per unit energy of finding a particle of energy E_G for a 1D gas at temperature T_G is

$$\frac{dP(E_G)}{dE_G} = \frac{1}{k_B T_G} \exp\left(-\frac{E_G}{k_B T_G}\right). \quad (10)$$

The 1D Knudsen flux gives an average energy of $\langle E_G \rangle = k_B T_G$, thus the energy accommodation coefficient is

$$\alpha(T_S, T_G) = \frac{\overline{E_f} - k_B T_G}{k_B T_S - k_B T_G}. \quad (11)$$

The average final energy $\overline{E_f}$ in Eqs. (9) and (11) is given by

$$\overline{E_f} = \int_0^\infty dE_G \int_0^\infty dE'_f E'_f \frac{dR(E'_f, E_G)}{dE'_f} \frac{dP(E_G)}{dE_G}. \quad (12)$$

The equilibrium energy accommodation coefficient (EAC) $\alpha_E(T)$, which is the form used for all calculations shown here, is defined as the limit in which T_S approaches T_G of Eq. (11),

$$\alpha_E(T) = \lim_{T_G \rightarrow T_S \rightarrow T} \frac{\overline{E_f} - k_B T_G}{k_B T_S - k_B T_G}. \quad (13)$$

The form can be simplified by making use of detailed balancing which relates the differential reflection coefficients

for the scattering interaction in which a particle makes the state-to-state transition $E_i \rightarrow E_f$ to that for $E_f \rightarrow E_i$ and is given by

$$\frac{dR(E_G, E_f)}{dE_G} = \frac{dR(E_f, E_G)}{dE_f} e^{(E_f - E_G)/k_B T_S}. \quad (14)$$

It can readily be shown that the differential reflection coefficient of Eq. (1) obeys the detailed balancing condition of Eq. (14).

Equation (14), together with the similar detailed balancing relation obeyed by the Knudsen flux of Eq. (10) allow the EAC to be expressed in the following form:

$$\alpha_E(T) = \frac{1}{2(k_B T)^2} \int_0^\infty dE_G \int_0^\infty dE_f (E_f - E_G)^2 \times \frac{dP(E_G)}{dE_G} \frac{dR(E_f, E_G)}{dE_f}. \quad (15)$$

For the iterative procedure described above in Sec. II B, Eq. (15) gives the partial equilibrium energy accommodation coefficient $\alpha_{EC}^n(T)$ due to the initially scattered fraction and all subsequently desorbed particles through the n th iteration which is expressed as

$$\alpha_{EC}^n(T) = \frac{1}{2(k_B T)^2} \int_0^\infty dE_G \int_D^\infty dE'_f (E'_f - E'_G)^2 \times \frac{dP(E_G)}{dE_G} \frac{dR^n(E'_f, E'_G)}{dE'_f}. \quad (16)$$

If one makes the classic assumption that the remaining trapped particles desorb with an equilibrium distribution and thus have an effective accommodation coefficient of unity, the corresponding EAC will be obtained by adding P_T^n to the right-hand side of Eq. (16).

The fully converged EAC is obtained by continuing the iteration process to the point where the trapped fraction P_T^n is an acceptably small number, and it is expressed by

$$\alpha_E(T) = \lim_{n \rightarrow \infty} \alpha_{EC}^n(T). \quad (17)$$

It is of interest to determine the energy distribution of the continuum fraction after the n th iteration which is given by

$$\frac{dP_C^n(E_f)}{dE_f} = \int_0^\infty dE_G \frac{dR^n(E'_f, E'_G)}{dE'_f} \frac{dP(E_G)}{dE_G}, \quad E_f > 0 \quad (18)$$

and the energy distribution of the trapped fraction is

$$\frac{dP_T^n(E_f)}{dE_f} = \int_0^\infty dE_G \frac{dR^n(E'_f, E'_G)}{dE'_f} \frac{dP(E_G)}{dE_G}, \quad -D < E_f < 0. \quad (19)$$

The energy distribution of all initially trapped and then subsequently desorbed particles is given by Eq. (18) with the 0th order contribution subtracted off.

D. Desorption time

It is also of interest to estimate the average desorption time of the initially trapped particles. There are clearly many

ways to make such an estimate given the energy distribution of the trapped fraction. Perhaps the simplest is to first determine either the average speed \bar{v}^n or the root mean square (rms) speed v_{rms}^n of the trapped particles after each iteration n . These are given by

$$\bar{v}^n = \frac{\int_0^\infty dE_G \int_{-D}^0 dE_f \sqrt{\frac{2E'_f}{m}} \frac{dP(E_G)}{dE_G} \frac{dR_T^n(E'_f, E'_G)}{dE'_f}}{P_T^n} \quad (20)$$

and

$$v_{\text{rms}}^n = \sqrt{\frac{\frac{2}{m} \int_0^\infty dE_G \int_{-D}^0 dE_f E'_f \frac{dP(E_G)}{dE_G} \frac{dR_T^n(E'_f, E'_G)}{dE'_f}}{P_T^n}}. \quad (21)$$

Estimates of the desorption time τ are then given by using either of the above average speeds in the following:

$$\tau = \sum_n \frac{2b P_T^n}{v^n P_T^0}, \quad (22)$$

where b is the width of the well.

III. RESULTS

Presented in this section are a number of calculations based on the theory developed in Sec. II. These calculated results are divided into three categories. The first of these concerns calculations of the energy distributions of both scattered and trapped particles, resulting from a flux of atoms incident on the surface. Two incident flux distributions are considered in Sec. III A, a monoenergetic incident beam and an incident equilibrium distribution of gas atoms. Section III B involves calculations of the energy accommodation coefficient and how its various components evolve with trapping and desorption of gas atoms. The third of these categories, Sec. III C, gives calculations of the rms speed, the average speed and the desorption time for the trapped fraction.

A. Incident energy distributions

First, we consider the situation in which a monoenergetic atomic beam is directed towards the surface. The initial scattering distribution is described by Eq. (1). The eventual desorption of the trapped particles is calculated with the iteration process described by Eqs. (3)–(8). Figure 1 shows an example for a mass ratio $\mu=0.22$ corresponding to Ar scattering from a tungsten target. The well depth is taken to be $D=40$ meV, the surface temperature is 300 K, and the incident beam energy is 2.8 meV. This is a plot of the differential reflection coefficient of Eq. (3) as a function of E_f . The range of negative values, $-D < E_f < 0$, shows the energy distribution of the trapped fraction, and $E_f > 0$ shows the distribution for the fraction of particles that have escaped from the surface. The solid curve shows the scattered differential reflection coefficient after the initial collision, i.e., after the 0th

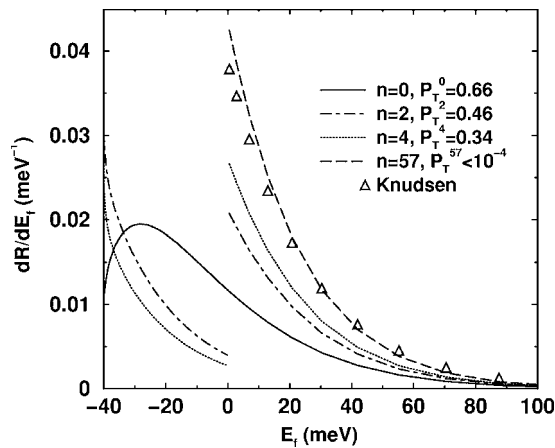


FIG. 1. The distribution of scattered particles as a function of the final energy for a monoenergetic incident beam. The mass ratio μ is 0.22, the temperature of the surface T is 300 K, the well depth D is 40 meV and the incident energy $E_i=2.8$ meV.

iteration. In this case the majority of the incident flux is trapped, with the trapped fraction $P_T^0=0.66$. A tail of atoms with fraction $P_C^0=1-P_T^0$ has escaped into the continuum with $E_f>0$, and the distribution curve is continuous as it crosses the boundary between continuum and trapped regions. The distribution of the continuum fraction deviates substantially from the Knudsen distribution shown as triangle symbols.

The dashed-dotted curve in Fig. 1 shows the situation after two more iterations. The fraction remaining in the trapped state has reduced to $P_T^2=0.46$. There is now, evidently, a discontinuity in the trapped and continuum distributions at the attractive well boundary. The dotted curve shows the situation after four iterations when the trapped fraction has further reduced to $P_T^4=0.34$, while the continuum distribution has become even larger.

The dashed curve gives the results after a large number of iterations for which nearly all of the trapped fraction has escaped. To characterize the situation in which nearly all particles have desorbed, an arbitrary cutoff of the iteration process was taken to be when the trapped fraction became less than 10^{-4} , which in this case took 57 iterations. At this point it is apparent that the total differential reflection coefficient, consisting of the sum of the initially scattered plus all desorbed particles, is not a Knudsen distribution at the surface temperature. At large final energies the calculated distribution function is smaller than the equilibrium distribution, while at low final energies the calculated distribution is larger.

Figure 2 shows a calculation for the same system but at the much higher incident energy of $E_i=70.5$ meV. As opposed to the case of Fig. 1 where the incident energy was small compared to the well depth, in this case the energy is large compared to D . The behavior of the distributions both inside and outside the well is similar to that of Fig. 1, but the initially trapped fraction is less than half, $P_T^0=0.33$. The trapped fraction decreases rapidly, with $P_T^2=0.22$ and $P_T^4=0.16$, but it still takes somewhat more than 50 iterations to reduce the trapped fraction to less than 10^{-4} . Again it is clear that the final converged energy distribution as shown by the

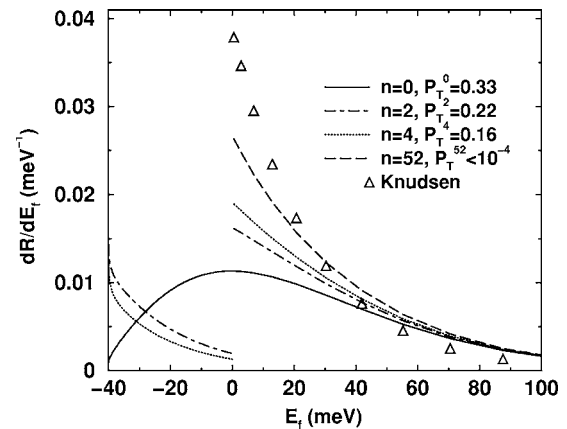


FIG. 2. Same as Fig. 1 except that the incident energy E_i is 70.5 meV.

dashed curve does not approach a Knudsen equilibrium distribution. However, in this case the calculated distribution is larger than the Knudsen curve at large final energies and smaller at low energies.

A large number of calculations have been carried out, of which typical examples are shown in Figs. 1 and 2 for wide ranges of the available parameters, namely D , E_i , μ , and T_S . In general, the conclusion is that neither the directly scattered contribution, i.e., the zeroth order iteration of Eq. (1), nor the trapped-desorbed contribution is well described by an equilibrium distribution. However, in the case of larger mass ratios μ and incident energies small compared to the well depth D the total scattered distribution (direct plus trapped-desorbed fractions) does approach a Knudsen distribution at the temperature of the surface.

Next we consider a quite different incident atomic distribution, an equilibrium gas that has an incident flux having the same temperature as the surface. Such a flux is described by the Knudsen distribution of Eq. (10), and this case will be of particular interest for calculations of the equilibrium energy accommodation coefficient discussed in Sec. II C above. Under these conditions detailed balancing indicates that the total backscattered distribution will also be in equilibrium with the surface temperature, as long as there are no anomalous processes acting such as chemisorption or other true sticking of incoming atoms. After the initial collision, however, that fraction of the incoming particles that are immediately scattered back into the continuum is not expected to be an equilibrium distribution. Similarly, the fraction that is initially trapped and then subsequently desorbed is also not necessarily expected to be an equilibrium distribution. It is the sum of all particles escaping from the surface, the initially scattered plus all desorbed particles, that is expected to make up the equilibrium distribution.

This behavior is shown in the examples of Figs. 3 and 4. Figure 3 is similar to and for the same parameters as Fig. 1 except that the incident beam is an equilibrium Knudsen distribution instead of monoenergetic. The initially trapped fraction is $P_T^0=0.54$ and after two more iterations is reduced to $P_T^2=0.37$. After a large number of iterations, in this case it takes $n=55$ to reduce the trapped fraction to below 10^{-4} , the continuum distribution shown as a dashed curve becomes

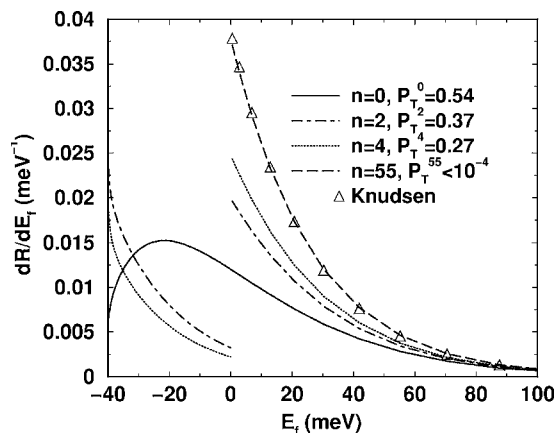


FIG. 3. The distribution of scattered particles as a function of the final energy for an equilibrium incident gas. $\mu=0.22$, $D=40$ meV, and $T=300$ K.

very nearly equal to the Knudsen distribution shown as triangle points.

Figure 4 shows the same Ar on tungsten system except that the well depth has now been chosen to be $D=100$ meV. In this case the initially trapped fraction is quite large, $P_T^0=0.79$, and the initially scattered fraction is small. After four more iterations the trapped fraction has decreased only by a small amount to $P_T^4=0.70$ and the continuum distribution is still quite far away from an equilibrium distribution at the surface temperature. However, after 515 iterations, when the trapped fraction drops to below the 10^{-4} threshold, the scattered distribution again is very close to a Knudsen distribution.

For the case of an equilibrium incident gas, we have carried out a number of calculations for wide ranges of all parameters. In most cases with $\mu < 1$ the total scattered distribution approaches very nearly to a Knudsen function, as expected. This result, of course, leads to an immediate consequence for the behavior of the trapped-desorbed fraction. The initially scattered distribution is not at equilibrium. As can be seen from the form of Eq. (1), it resembles more a skewed Gaussian function (except for very low incident energies, where its behavior becomes exponential with argument $-4\mu E_f/[T(1+\mu)^2]$), but it is still not a Knudsen func-

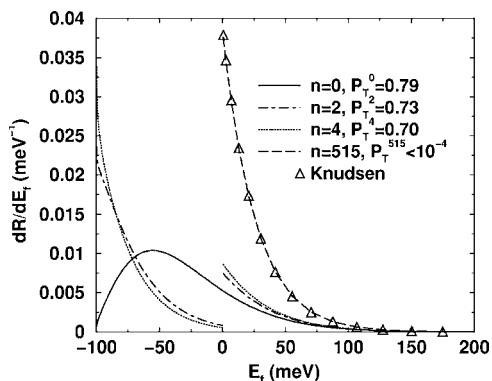


FIG. 4. Same as Fig. 3 except that the well depth is changed to 100 meV.

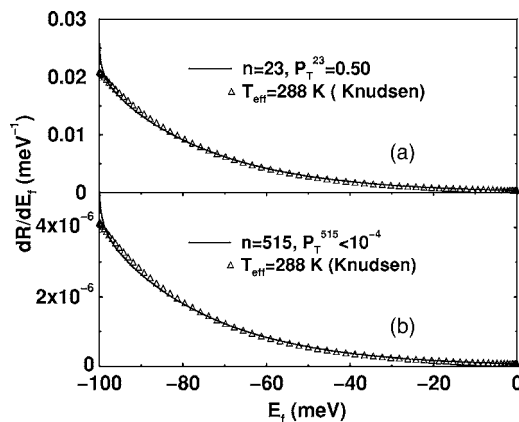


FIG. 5. For the same conditions as in Fig. 4, the distribution of bound particles after two different numbers of iterations, (a) $n=23$ with $P_T^{23}=0.50$ and (b) $n=515$ with $P_T^{515} < 10^{-4}$.

tion). Thus, if the total scattered distribution is of Knudsen form, and the initially scattered fraction is not, then the trapped-desorbed fraction is in general also not a Knudsen function. Thus, not only for the case of a monoenergetic incident beam, but also for an equilibrium incident flux, the trapped-desorbed fraction does not in general escape at equilibrium with the surface. This will become more apparent in the discussion of the energy accommodation coefficient in Sec. III B below.

It is of interest to discuss the energy distribution of the fraction of incident particles that are trapped in the well and how this distribution evolves as a function of multiple collisions in the well. As mentioned above, it is found that the trapped particle distribution function typically stabilizes after a relatively small number of iterations and then remains constant thereafter. This stable bound state distribution resembles an equilibrium distribution, but usually at a temperature lower than that of the surface. Figure 5 gives more detail on the energy distribution of trapped particles for the same system shown in Fig. 4, i.e., an incident equilibrium flux of Ar in contact with a tungsten surface with $D=100$ meV and $T=300$ K, and compares the distribution to a Knudsen distribution after two different iteration numbers. After 23 iterations, Fig. 5(a) shows the fraction remaining trapped is 0.50, and the distribution is shown by the solid curve. The distribution compares well with a Knudsen distribution shown as triangle points with a temperature of 288 K, somewhat lower than the surface temperature of 300 K. However, at low energies below 60 meV near the bottom of the well, a least squares fit between a Knudsen distribution and the calculations gives a temperature of 300 K, exactly that of the surface. This indicates that the escaping particles come from near the top of the well, thus reducing the effective temperature, while those particles near the bottom of the well come into near equilibrium with the surface.

The functional form exhibited in Fig. 5(a) is arrived at after a relatively small number of iterations and then remains essentially unchanged for all subsequent iterations. The only change is that the total fraction of trapped particles continues to decrease, roughly exponentially. This behavior is shown in Fig. 5(b), which is similar to Fig. 5(a) except that the trapped

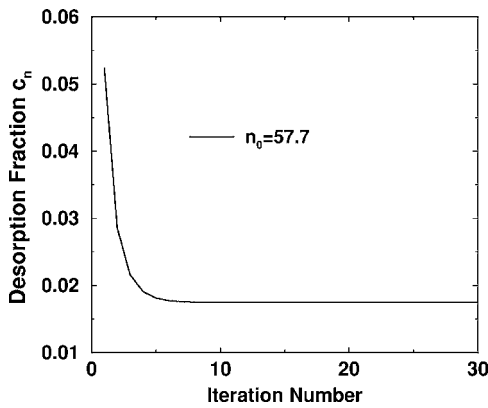


FIG. 6. The desorption fraction as a function of iteration number for the equilibrium incident gas of Fig. 4.

fraction is now 10^{-4} after a total of $n=515$ iterations. The calculated curves in Figs. 5(a) and 5(b) are nearly identical, and both are well matched by the Knudsen distribution with a temperature of 288 K. This behavior also implies that after a certain number of iterations the functional form of the desorbed contributions coming from each iteration stabilizes into a well-defined partial differential reflection coefficient.

The tendency of the trapped distribution to stabilize after a certain number of iterations has important implications. It means that, after this stability has been achieved, all subsequently desorbed particles leave the surface with the same energy distribution. The desorption fraction c_n of the trapped particles after the n th iteration is

$$c_n = \frac{P_T^{n-1} - P_T^n}{P_T^{n-1}}. \quad (23)$$

c_n initially changes with the iteration number but eventually converges to a nearly constant value c for large n .

When the iteration number is large, the fraction of particles left in the well decreases with iteration number according to the relation

$$P_T^n = P_T^{n_1} (1 - c)^{n-n_1}, \quad n > n_1, \quad (24)$$

where n_1 is the threshold value above which $c_n \approx c$.

In Fig. 6, the conditions are the same as in Fig. 5. The solid curve illustrates how the desorption fraction c_n changes with iteration number. It is obvious that the desorption fraction approaches a constant value after only a few iterations.

When c is small, Eq. (24) can be written approximately as an exponential function

$$P_T^n = P_T^{n_0} \exp\left\{-\frac{n}{n_0}\right\}, \quad n > n_0, \quad (25)$$

where $c=1/n_0$, and for the case of Figs. 5 and 6 $n_0=57.7$.

This stabilization behavior of the trapped distribution is quite general, and occurs regardless of the form of the incident flux or the other parameters. The rate at which this stable distribution function forms depends mainly on the initially trapped fraction. For small initially trapped fractions the stable behavior arrives after just a small number of iterations, while for large trapped fractions it takes a larger num-

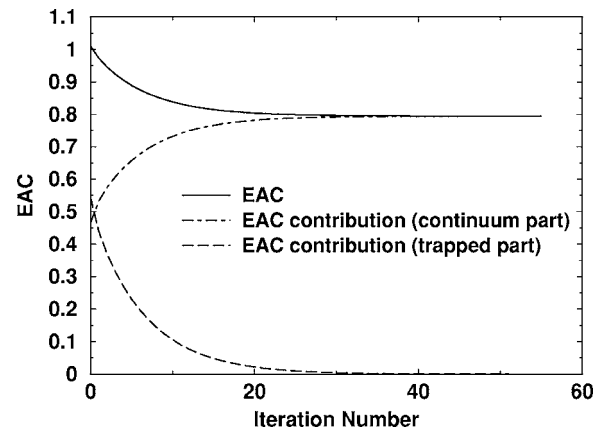


FIG. 7. The evolution with iteration number n of the three contributions to the EAC for $T=300$ K.

ber of iterations and the decay constant n_0 is large.

This immediately suggests ways that the calculation algorithm can be adapted to this stationary state behavior in order to speed up the calculation after a stable configuration has been achieved. Although in this treatment all calculations were carried out completely using the iteration method, exploitation of the eventual stability of the distribution, and its resultant exponential behavior as expressed in Eq. (25), may be very useful for calculations involving heavier atoms with deep physisorption wells where trapping times are long and the number of iterations becomes quite lengthy. It could also be useful in the case in which similar methods are used for calculating scattering and trapping in a full 3D potential, or for the case of molecular projectiles which have internal degrees of freedom that must be taken into account in the scattering process.

B. Accommodation coefficient

General results for the iterative scattering process applied to the behavior of the equilibrium energy accommodation coefficient (EAC) are shown in Figs. 7 and 8. The general behavior is that the EAC starts off with an initially higher

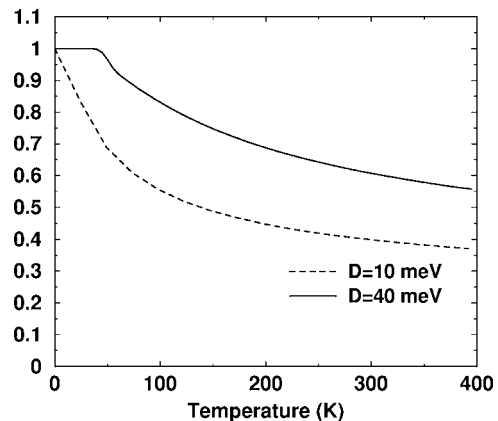


FIG. 8. The EAC contribution given by all initially trapped particles as a function of the temperature for two different well depths. μ is 0.22.

value and then with increasing iteration number it saturates to a lower value. However, this appearance is due to the assumption that the trapped particles have an effective EAC of unity, as will become more apparent from an examination of Fig. 7. The saturated values, occurring at large iteration number, are independent of any assumption about the initially trapped fraction because at that point all particles have desorbed and the EAC is determined with the fully converged continuum scattered distribution. The saturated value of the EAC is usually achieved to better than 1% when the trapped fraction becomes less than 0.01. For all further calculations presented here, the saturated value of the EAC is given when $P_T < 10^{-4}$.

As a function of temperature the saturated EAC values decrease with increasing T . This is the expected behavior and is in agreement with most experimental observations.⁶⁻⁹ It is also clear that the iteration process converges much more quickly at high temperatures than for lower temperatures. Again, this is as expected since desorption times are expected to be shorter at higher temperatures.

Figure 7 gives the evolution of the various contributions to the EAC. The mass ratio is chosen to be $\mu=0.22$ corresponding to Ar scattering from a W surface, the well depth is $D=40$ meV and the temperature is 300 K. The solid curve gives the EAC as a function of iteration number under the assumption that the trapped particles escape with an effective AC of unity. The dashed-dotted curve is the EAC calculated with the differential reflection coefficient of the continuum fraction only, with no contribution from those particles that remain trapped. Both of these two curves must approach the same final value at large iteration number. The dashed curve is the calculated AC contribution of the trapped fraction using the assumption that the trapped fraction has an effective accommodation coefficient of unity at each iteration. This decreases as the trapped fraction becomes smaller and consequently approaches zero.

The important and fundamental question of how trapped particles contribute to the EAC is addressed in Fig. 8. Plotted as a function of temperature is the EAC calculated from the energy distribution of initially trapped and subsequently desorbed fraction of particles. The iteration process is fully converged and at all temperatures the values presented are for iteration numbers sufficiently large that the trapped fraction $P_T < 10^{-4}$. The conditions are the same as in Fig. 7 except that two different well depths, $D=10$ meV and $D=40$ meV, are shown. The contribution from trapped particles is the quantity that is usually assumed to be identically unity. It is seen clearly that this assumption is not necessarily correct. For the smaller well depth of 10 meV the EAC contribution from the trapped-desorbed fraction approaches unity only at very low temperatures, and at higher temperature it is less than unity. For the case of the deeper well of 40 meV, the EAC contribution of the trapped-desorbed particles is very nearly unity over a range of low temperatures. In that temperature range, nearly all of the incident flux is initially trapped. However, as the surface temperature, in energy units of $k_B T$, becomes larger with respect to the well depth the EAC contribution becomes smaller than unity. These typical curves represent the general behavior observed in calculations for the accommodation contribution of the

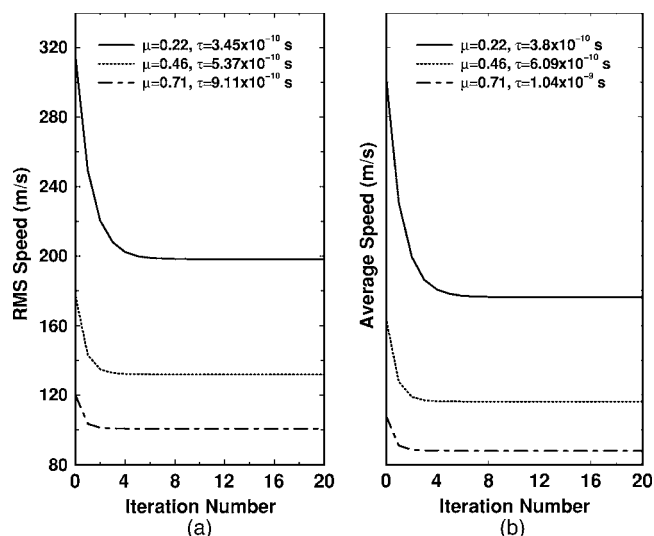


FIG. 9. (a) The root mean square speed as a function of the iteration number. (b) The average speed as a function of the iteration number. The well depth is $D=40$ meV, the temperature is $T=100$ K, and three different mass ratios are shown. τ is the calculated desorption time for the trapped particles.

trapped fraction. At low temperatures, the trapped contribution can be large but eventually it decreases monotonically with T . The contribution is larger the deeper the well depth. The temperature and well depth behavior are consistent with the general prediction that the longer the trapping time, the larger will be the contribution of the trapped fraction to the full EAC. These calculations indicate that the assumption that the trapped-desorbed fraction leaves in equilibrium with the surface is not necessarily the general case.

As a final note in the discussion of the EAC, we have made no attempt to exhibit here a figure of the comparison of our calculations with available experimental data. The reason for this, as discussed above, is the limitations of one-dimensional models to describe the three-dimensional case under which the measurements are made. As has been discussed before, 1D models have a tendency to overestimate the EAC, and such is the case here. However, the general qualitative aspects of the measured data for rare gases accommodating at metal surfaces are exhibited by these calculations. In particular, it is found that the EAC at a given temperature increases with increasing mass ratio μ , and for fixed μ it is a monotonically decreasing function of the temperature T .

C. Desorption time

As discussed above in connection with Eqs. (20)–(22) the iteration approach to calculating desorption provides a convenient way of estimating desorption times. Basically, the method suggested is to use the bound state energy distributions after each iteration to calculate either an average speed or an rms speed at each iteration. Then, knowing the width of the well, the time required to remove essentially all the trapped particles is a simple calculation. An example illustrating this process is shown in Fig. 9. As a function of

iteration number n , this shows the calculated rms speed and average speed of the trapped particles for three different mass ratios all at a temperature of 100 K assuming an equilibrium incident flux. In comparison with the earlier calculations shown in Fig. 7 for the EAC as a function of iteration number, it is evident that the rms and average speeds stabilize for much smaller iteration numbers than required to get a fully saturated EAC. This again is an indication that the energy distribution of particles in the well stabilizes after relatively few iterations. The calculated desorption times, based on a well width of $b=3 \text{ \AA}$, are also given in Fig. 9. Desorption times τ range from 3.5×10^{-10} s for a mass ratio of 0.22 to 1.04×10^{-9} s for the larger value of $\mu=0.71$.

IV. CONCLUSIONS

The scattering process naturally divides into four different components, all described in terms of a differential reflection coefficient or energy distribution, (1) the initially scattered fraction, (2) the initially trapped fraction, (3) the energy distribution of the subsequently desorbed fraction after suffering multiple collisions inside the well, and (4) the energy distribution of the remaining trapped particles before they eventually desorb. It is the latter two contributions that are described by the iteration process.

Although one-dimensional models are not adequate for describing experimental data obtained in a real three-dimensional scattering apparatus, very useful qualitative information is obtained from these calculations. In particular, we are able to address the question of whether initially trapped particles, after many collisions with the surface while traveling in the well, eventually desorb in an equilibrium distribution at the temperature of the surface. What we find is that such an assumption is not valid in general. For systems having very deep wells, high gas to surface mass ratios, and at low temperatures, all conditions for which the desorption time is long, the initially trapped and subsequently desorbed fraction approaches an equilibrium distribution. However, in general the desorbed fraction leaves the surface with a distribution that is not in equilibrium. This behavior is also reflected in calculations of the energy accommodation coefficient. If the particles desorb in an equilibrium distribution then their partial contribution to the EAC should be unity (i.e., equal to the fraction of desorbed particles), but it is found that, except for the systems with large D and μ and small T , the desorbed contribution to the EAC is less than unity and sometimes significantly less.

The equilibrium accommodation coefficient is a useful concept from which to discuss gas-surface dynamics, especially in view of the fact that the current calculations are one dimensional and 1D models have a long and important history in EAC calculations. We find that the EAC, calculated including the trapped-desorbed fraction, converges in general to smaller values than would be obtained by just using the differential reflection coefficient based on only a single collision with the surface. This is because the fractional EAC contributed by the trapped-desorbed particles is typically less than unity, contrary to the usual assumption. It is also of interest to discuss the distribution of scattered gas particles

resulting from an equilibrium incident flux, i.e., the case for which the EAC is calculated, and for which the scattered distribution should also be an equilibrium flux. We find, not surprisingly, that the initial scattered fraction after a single collision with the surface is not a Knudsen distribution. The subsequently desorbed fraction also leaves the surface with a non-Knudsen distribution. However, the sum of the two, the total distribution of scattered particles is, as expected, a Knudsen distribution at the temperature of the surface. The iterative formalism presented here clearly shows how the final equilibrium distribution develops with increasing numbers of desorbed particles.

The iteration method allows one to examine the energy distribution of the fraction of particles trapped in the well, and to follow the functional form of this distribution as the particles desorb. After a relatively small number of iterations, as compared to the number required to desorb essentially all trapped particles, the trapped energy distribution takes on a constant functional form with only the total trapped fraction decreasing in an approximately exponential decay. Once the trapped distribution has stabilized, and the subsequent desorption is approximately exponential, this behavior can be used as an approximation for calculating the subsequently desorbed particles without continuing the iteration process. Such an exponential approximation, although not exploited here, could be useful in situations where the number of iterations becomes large or where the interaction potential becomes more complicated or higher dimensional.

Because the energy distribution of trapped particles is calculated at every iteration, we are able to calculate the desorption time, or equivalently the average time a particle remains trapped. Several different estimates of the desorption time can be calculated, and two are suggested based on using the trapped energy distribution to calculate the average or rms speed of bound particles. It is found that as a function of iteration number, the average or rms speed quickly saturates to a constant value. This is another indication of the stabilization of the trapped energy distribution after a small number of iterations.

Finally, we come to a brief discussion of the extension of the present calculations to real three-dimensional scattering systems. Initial calculations have been carried out for three-dimensional scattering kernels which are extensions of that used here in Eq. (1).¹⁶ The time consuming part of the 1D calculations presented here is carrying out a triple integral at each iteration. For a 3D model this becomes a ninth order integral at each iteration. However, the initial calculations show that the 3D case can be treated even when the number of iterations required is large. Also, this is a situation in which the stabilization of the trapped distribution after a small number of iterations can be exploited by use of exponential approximations to calculate the remaining desorbed distribution.

ACKNOWLEDGMENTS

This work was supported by the National Science Foundation under Grant No. DMR-0089503 and by the Department of Energy under Grant No. DE-FG02-98ER45704.

- ¹J. C. Maxwell, *Philos. Trans. R. Soc. London* **170**, 251 (1879).
- ²M. Knudsen, *The Kinetic Theory of Gases*, 3rd ed. (Wiley, New York, 1950), p. 47.
- ³S. C. Saxena and R. K. Joshi, "Thermal accommodation and adsorption coefficient of gases," in *CINDAS Data Series on Material Properties*, edited by C. Y. Ho (Hemisphere, New York, 1989).
- ⁴Frank O. Goodman and Harold Y. Wachman, *Dynamics of Gas-Surface Scattering* (Academic, New York, 1976), p. 255.
- ⁵A. Özer and J. R. Manson, *Surf. Sci.* **502-503**, 352 (2002).
- ⁶L. B. Thomas, in *Rarefied Gas Dynamics*, edited by C. L. Brundin (Academic, New York, 1967), p. 155.
- ⁷L. B. Thomas, in *Fundamentals of Gas-Surface Interactions*, edited by H. Saltzburg, J. N. Smith, Jr., and M. Rogers (Academic, New York, 1967), p. 346.
- ⁸J. Kouptsidis and D. Menzel, *Z. Naturforsch. A* **24A**, 470 (1969).
- ⁹J. Kouptsidis and D. Menzel, *Ber. Bunsenges. Phys. Chem.* **74**, 512 (1970).
- ¹⁰A. Sjölander, *Ark. Fys.* **14**, 315 (1959).
- ¹¹D. A. Micha, *J. Chem. Phys.* **74**, 2054 (1981).
- ¹²A. Muis and J. R. Manson, *J. Chem. Phys.* **111**, 730 (1999).
- ¹³J. Dai and J. R. Manson, *J. Chem. Phys.* **119**, 9847 (2003).
- ¹⁴Andre Muis and J. R. Manson, *Phys. Rev. B* **54**, 2205 (1996).
- ¹⁵J. Powers, J. R. Manson, C. E. Sosolik, J. R. Hampton, A. C. Lavery, and B. H. Cooper, *Phys. Rev. B* **70**, 115413 (2004).
- ¹⁶Guoqing Fan and J. R. Manson (unpublished).